A loss of function allele for murine Staufen1 leads to impairment of dendritic Staufen1-RNP delivery and dendritic spine morphogenesis

John P. Vessey*[†‡], Paolo Macchi*[†‡§], Joel M. Stein[‡¶], Martin Mikl[†], Kelvin N. Hawker[‖**], Petra Vogelsang*[††], Krzysztof Wieczorek[†], Georgia Vendra[†], Julia Riefler[†], Fabian Tübing*[†‡‡], Samuel A. J. Aparicio[‖§§], Ted Abel[¶], and Michael A. Kiebler*[†¶¶]

*The-Max Planck Institute for Developmental Biology, Spemannstrasse 35, D-72076, Tübingen, Germany; [†]Center for Brain Research, Medical University of Vienna, Spitalgasse 4, A-1090 Vienna, Austria; [¶]Department of Biology, University of Pennsylvania, Philadelphia, PA 19104; and [‖]Cambridge Institute for Medical Research, Wellcome Trust/MRC Building, Department of Oncology, Hills Road, Cambridge, CB2 2XY, United Kingdom

Edited by Ruth Lehmann, New York University Medical Center, New York, NY, and approved September 5, 2008 (received for review May 12, 2008)

The dsRNA-binding protein Staufen was the first RNA-binding protein proven to play a role in RNA localization in *Drosophila*. A mammalian homolog, Staufen1 (Stau1), has been implicated in dendritic RNA localization in neurons, translational control, and mRNA decay. However, the precise mechanisms by which it fulfills these specific roles are only partially understood. To determine its physiological functions, the murine Stau1 gene was disrupted by homologous recombination. Homozygous *stau1*^{tm1Apa} mutant mice express a truncated Stau1 protein lacking the functional RNA-binding domain 3. The level of the truncated protein is significantly reduced. Cultured hippocampal neurons derived from *stau1*^{tm1Apa} homozygous mice display deficits in dendritic delivery of Stau1-EYFP and *β-actin* mRNA-containing ribonucleoprotein particles (RNPs). Furthermore, these neurons have a significantly reduced dendritic tree and develop fewer synapses. Homozygous *stau1*^{tm1Apa} mutant mice are viable and show no obvious deficits in development, fertility, health, overall brain morphology, and a variety of behavioral assays, e.g., hippocampus-dependent learning. However, we did detect deficits in locomotor activity. Our data suggest that Stau1 is crucial for synapse development *in vitro* but not critical for normal behavioral function.

dendrite | RNA transport | ribonucleoprotein particles | double-stranded RNA-binding protein

Protein synthesis-dependent synaptic plasticity is considered a fundamental mechanism facilitating learning and memory in the central nervous system. Local translation of mRNA stored in dendrites has emerged as an important mechanism contributing to this synapse-specific event (1–2). Although a number of components have been recently implicated in dendritic mRNA localization, the underlying molecular mechanisms are only partially understood. A key protein involved in this process is Staufen, a dsRNA-binding protein originally identified in *Drosophila* (3). *Drosophila* embryos lacking Staufen exhibit anterior head defects, deletions of abdominal segments, and a lack of germ cell formation resulting from the mislocalization of *oskar* and *bicoid* mRNA (4). Interestingly, a recent study implicated *Drosophila* Staufen in long-term memory formation (5).

In mammals, the function of the two mammalian Staufen proteins, termed Stau1 and Stau2, is much less clear. Both Staufen proteins are components of RNPs that travel along microtubules from the soma to distant dendritic sites. Whereas Stau1 is thought to function in translational control and mRNA decay (6, 7), the brain-specific Stau2 has been implicated in mRNA transport (8) and dendritic spine morphogenesis (9). To address the role of the mammalian Staufen1 protein *in vivo*, we developed a loss of function allele in murine *Stau1* using gene targeting. This allowed us to determine whether the lack of Stau1 affects neuronal granule assembly, synapse formation, or learning and memory.

Results and Discussion

Targeted Disruption of the *Stau1* Gene Leads to a Mutant Stau1 Protein Deficient in RNA-Binding. To generate a loss of function allele in *Stau1*, we inserted an IRESβgeo cassette into exon 5 (10). This exon encodes for most of the dsRNA-binding domain 3 (dsRBD3), which is crucial for RNA-binding (11). Translation of any truncated 5′ transcript would result in dsRBD1 and dsRBD2 and lack the critical functions encoded by dsRBD3. The targeting vector introduces a translational stop upstream of the IRES sequence and a cassette with a polyA into the BglII site of exon 5 (Fig. 1*A*). This allele was designated *stau1*^{tm1Apa} (12). Targeting was carried out in 129SvEv (129S7) ES cells. This was verified via Southern blotting using a 5′ external probe (Fig. 1*B Bottom*) and by 3′ PCR (Fig. 1*B Top*) using primers stauR5 and neo236, yielding a 2.9kb PCR product. Two correctly targeted clones were selected that transmitted through the germline. The F1 founders were backcrossed once to parental 129SvEv mice before intercrossing. The resulting *stau1*$^{tm1Apa/tm1Apa}$ mice were viable, reproduced normally, and showed no obvious anatomical abnormalities [supporting information (SI) Fig. S1]. Mice were genotyped by multiplex PCR as shown in Fig. 1*C*.

To determine the effect of the stau1^{tm1Apa} allele on expression of Stau1 protein, forebrain extracts were prepared from both WT and homozygous stau1^{tm1Apa} mice and subjected to Western blotting. Probing with an immunopurified polyclonal anti-Stau1 antibody (13) revealed a truncated Stau1 protein of ≈50 kDa that is substantially reduced in expression levels (Fig. 1*D*). No protein of predicted full-length was observed. In contrast, Stau2

Author contributions: J.P.V., P.M., J.M.S., M.M., K.N.H., K.W., G.V., S.A.J.A., T.A., and M.A.K. designed research; J.P.V., P.M., J.M.S., M.M., K.N.H., P.V., K.W., J.R., and F.T. performed research; J.P.V., P.M., J.M.S., M.M., K.N.H., P.V., K.W., G.V., J.R., F.T., S.A.A., T.A., and M.A.K. analyzed data; and J.P.V. and M.A.K. wrote the paper.

The authors declare no conflict of interest.

This article is a PNAS Direct Submission.

Freely available online through the PNAS open access option.

[‡]J.P.V., P.M., and J.M.S. contributed equally to this work.

[§]Present address: Centre for Integrative Biology, University of Trento, Via delle Regole 101, 38060 Mattarello, Italy.

**Present address: NCIP Ropewalk House, 113 The Ropewalk, Nottingham NG1–6HA, UK.

[††]Present address: Broegelmann Research Laboratory, The Gade Institute, University of Bergen, Haukelandsveien 28, N-5021 Bergen, Norway.

[‡‡]Present Address: Roche Diagnostics, TE-FC2, Nonnenwald 2, D-82377 Penzberg, Germany.

[§§]Present address: BC Cancer Agency, 675 West 10th Avenue, Vancouver, BC, Canada V5Z 1L3.

[¶¶]To whom correspondence should be addressed. E-mail: michael.kiebler@meduniwien.ac.at.

This article contains supporting information online at www.pnas.org/cgi/content/full/0804583105/DCSupplemental.

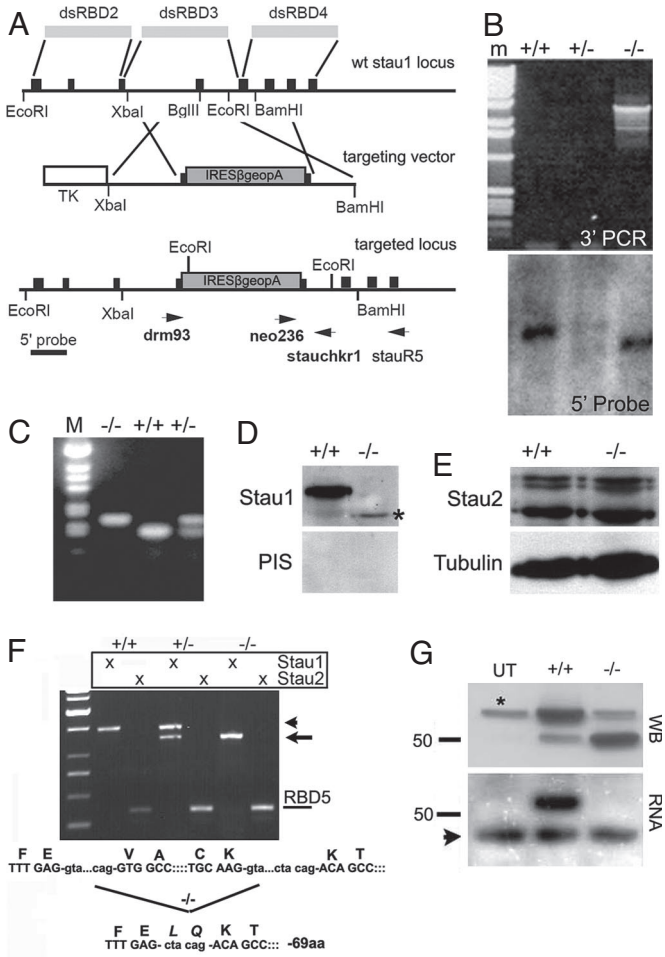

Fig. 1. Truncated stau1 lacking dsRBD3 leads to reduced Stau1 protein levels and an impairment of RNA-binding capacity. (*A*) Targeting strategy for disrupting the *Stau1* gene in mouse. WT genomic locus (*Top*) shows the location of the dsRBD3, the sites for homologous recombination with the targeting vector (IRESβgeopA, *Middle*) and the final targeted, mutated *Stau1* locus (*Bottom*). Arrowheads indicate the primers used for genotyping. 5′ probe, indicates the probe used for Southern blotting. (*B*) 3′ PCR (*Top*) and 5′ Southern blot (*Bottom*) analysis of WT (+/+), heterozygous (+/-), and mutant (−/−) Stau1 mice. For Southern blotting, genomic DNA was EcoRI-digested and probed with a PCR fragment (nt 325–568 of the Stau1 locus, 5′ probe). The DNA from stau1^{tm1Apa} homozygous mice (−/−) shows a 1.5 kb deletion (from 10 to 8.5 kb) due to the presence of an additional EcoRI site in the recombinant locus. For verification of 3′ targeting (*Top*, 3′ PCR), primers stauR5 and neo236 were used, generating a 2.9kbp PCR product in the correctly targeted clones. m, marker. (*C*) PCR genotyping indicating the two resulting PCR fragments for either WT (+/+) or stau1^{tm1Apa} homozygous mice (−/−). M, marker. (*D*) Western blot of WT (+/+) and stau1^{tm1Apa} (−/−) forebrain extracts probed with an immunopurified polyclonal anti-Stau1 antibody (*Upper*). In mutant brain, a faint band of lower molecular weight is visible (asterisk). The lower panel shows a blot probed with the preimmune serum (PIS) of the Stau1 rabbit. (*E*) Western blot of WT (+/+) and stau1^{tm1Apa} (−/−) forebrain extracts probed with an immunopurified polyclonal anti-Stau2 antibody or a monoclonal anti-tubulin antibody as internal loading control. Expression levels of the three Stau2 isoforms (62, 59, and 52 kDa, respectively) are unchanged. (*F*) Detection of full-length *Stau1* and *Stau2* mRNAs isolated from brains of WT (+/+), heterozygous (+/-), or stau1^{tm1Apa} homozygous mice (−/−) by RT-PCR. In contrast to WT (arrowhead), a shortened Stau1 transcript is found in stau1^{tm1Apa} homozygous mice caused by an in-frame deletion of 207 nts in RBD3 (arrow). As internal control, the dsRBD5 of Stau2 was amplified in parallel. The scheme below shows skipping of exon 5 in stau1^{tm1Apa} homozygous mice (−/−) leading to a deletion of 69 aa within the dsRBD3 (amino acids in italics, LQ is added in ΔStau1 due to alternative splicing). (*G*) ΔStau1 lacking RBD3 does not bind RNA *in vitro*. A Northwestern assay was performed on HeLa cell extracts transfected with WT (+/+) or ΔStau1 (−/−) and probed with an immunopurified polyclonal anti-Stau1 antibody (WB). The asterisk marks endogenous Stau1 protein in HeLa. Proteins were renatured on the filter and exposed to a synthetic ^{32}P-labeled poly rI/rC probe. Arrowhead indicates unspecific RNA binding to a protein present in all extracts. UT, untransfected control.

expression was not affected by the disruption of the *Stau1* locus (Fig. 1*E*). To further characterize the low level truncated protein, we isolated and sequenced mRNA from forebrains of stau1^{tm1Apa} homozygous mice. Transcripts isolated contain an in-frame deletion of 207 nucleotides (68 residues) coding for the dsRBD3 (Fig. 1*F*) as the result of skipping exon 5. We refer to this protein as ΔStau1. Since the dsRBD3 of Stau1 is crucial for RNA binding in *Drosophila* and mammals (11, 14), we next assessed the RNA-binding capacity of the ΔStau1 protein by a Northwestern assay. Untagged mouse Stau1 and ΔStau1 were expressed in HeLa cells at approximately equal levels (Fig. 1*G Top*). After renaturation of the blotted proteins, the nitrocellulose membrane was exposed to a synthetic ^{32}P-labeled poly(rI/rC) probe. Overexpressed Stau1 bound significant amounts of RNA (Fig. 1*G Lower*). A second band of lower molecular weight, presumably an endogenous RNA-binding protein comigrating with overexpressed ΔStau1 (Fig. 1*G*, arrowhead), prevents a conclusive statement regarding the RNA-binding capacity of the ΔStau1 protein. However, since this lower comigrating band is of the same relative intensity in all three lanes, we conclude that overexpressed ΔStau1 does not bind RNA to the same extent as overexpressed WTStau1.

Loss of WTStau1 Leads to Impairments in Dendritic RNP Localization. Although brain extracts from stau1^{tm1Apa} homozygous mice contained significantly reduced levels of Stau1 (Fig. 1*D*), we next asked whether any residual protein could be detected in hippocampal neurons. Both pyramidal neurons in the CA1 (Fig. 2*B*) as well as dissociated hippocampal neurons in culture (Fig. 2*D*) derived from stau1^{tm1Apa} homozygous mice fail to express significant amounts of Stau1 protein in contrast to their WT counterparts (Fig. 2 *A* and *C*). Staining of cultured neurons revealed that Stau2 is expressed at equal levels by both WT and stau1^{tm1Apa} homozygous mouse neurons in a particulate pattern in both the cell body and distal dendrites (Fig. S2*A*). Since *Drosophila* Staufen heterooligomerizes with itself and several copies of *oskar* mRNA to form functional RNA particles (11), we investigated whether ΔStau1-EYFP protein shows any impairment in particle formation and dendritic localization upon expression in both WT (Fig. 2*G*) or *stau1*^{tm1Apa} homozygous neurons (Fig. 2*H*). When WTStau1-EYFP was transfected into neurons derived from ΔStau1 mice (Fig. 2*F*), 68% of all transfected neurons display puncta in dendrites (Fig. 2*I*), compared to 83% when transfected into WT neurons (Fig. 2 *E* and *I*). The maximum distance that WTStau1-EYFP puncta could be detected from the cell soma in neurons lacking WTStau1 was 81.76 μm (Fig. 2*J*), not significantly different from when transfected into WT neurons (102.94 μm). In contrast, when ΔStau1-EYFP was transfected into neurons lacking Stau1, only 18% of all neurons displayed punctate EYFP expression in dendrites (Fig. 2 *H* and *I*). In those neurons that contained punctate ΔStau1-EYFP, the average maximum distance from the cell body was significantly reduced (45.25 μm to 102.94 μm, $P < 0.001$, Fig. 2*J*) compared to that of WTStau1-EYFP transfected into WT neurons. In summary, these data suggest that two functional copies of Stau1 are required for proper dendritic targeting of this protein. However, the presence of endogenous WTStau1 is sufficient to warrant particle formation and dendritic targeting of ΔStau1-EYFP as observed when this construct was transfected into WT neurons. Staufen proteins have the ability to

NEUROSCIENCE

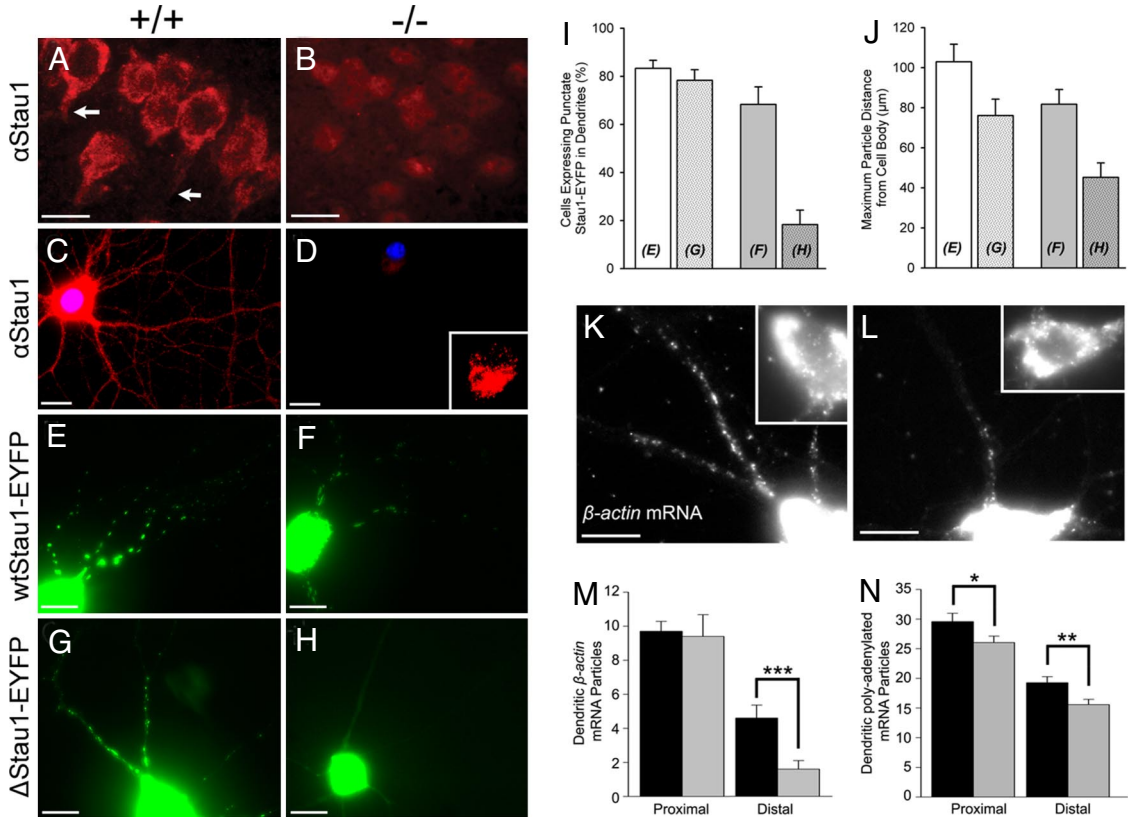

Fig. 2. Hippocampal neurons lacking WTStau1 show impaired RNP transport to distal dendrites. Neurons derived from WT mice are displayed on the left (*A, C, E, G,* and *K*) and those derived from stau1^{tm1Apa} homozygous mice on the right (*B, D, F, H,* and *L*). (*A and B*) stau1^{tm1Apa} homozygous mice do not express detectable amounts of Stau1. Immunocytochemistry on hippocampal slices using a polyclonal anti-Stau1 (αStau1) antibody shows that Stau1 is expressed in both cell bodies and dendrites (arrows) of WT mice but not of stau1^{tm1Apa} homozygous mice. (*C* and *D*) Cultured hippocampal neurons derived from stau1^{tm1Apa} homozygous mice do not express Stau1. Immunocytochemistry was performed on hippocampal neurons derived from WT or stau1^{tm1Apa} homozygous mice using a polyclonal anti-Stau1 antibody. Inset shows an enlargement of the cell body in *D* with little nuclear staining. Nuclei were visualized with DAPI. (*E* and *F*). WTStau1-EYFP forms particles that are transported into distal dendrites of hippocampal neurons derived from WT or stau1^{tm1Apa} homozygous mice. (*G* and *H*) ΔStau1-EYFP needs WTStau1 to form RNPs that are transported into distal dendrites. When WTStau1 is lacking, the ΔStau1-EYFP expression pattern is diffuse with few detectable particles in neuronal dendrites. (*I* and *J*) Quantification of the results obtained in *E, F, G,* and *H* (letters superimposed on each bar indicate the panel of the representative neuron from each condition). (*I*) When mutant ΔStau1-EYFP is transfected in neurons derived from stau1^{tm1Apa} homozygous mice, it results in a failure to form ΔStau1-containing RNPs (81.7 ± 6% SE, $P < 0.001$). In cases where ΔStau1-containing RNPs do form (*I,* 18.3 ± 6%, $P < 0.001$), (*J*) they are less prominent in distal dendrites as for WTStau1-GFP (45.2 ± 7.2 μm SE, versus 102.9 ± 8.7 μm SE from the cell body, $P < 0.001$). White bars represent neurons derived from WTStau1 mice; gray bars neurons from stau1^{tm1Apa} homozygous mice. White bars indicate neurons transfected with WTStau1-EYFP whereas dotted bars indicate neurons transfected with ΔStau1-EYFP. Neurons were fixed 24 h after transfection and their expression pattern was quantified. The maximum distance a WT or ΔStau1-EYFP particle could be detected in all puncta-expressing neurons was measured. (*K* and *L*) Detection of β-*actin* mRNA by FISH. Neurons derived from stau1^{tm1Apa} homozygous mice (*L*) show a reduction in the number of distal dendritic β-*actin* mRNPs compared to their WT counterparts (*K*). Lower exposure insets of the cell bodies reveal similar expression levels of β-*actin* mRNA in the soma. (*M* and *N*) Quantification of β-*actin* (*M*) and polyadenylated (*N*) mRNA particles. Proximal dendrites were considered as the first 25 μm, distal dendrites as the subsequent 25 μm of dendrite length. Black bars, WT neurons; gray bars, stau1^{tm1Apa} homozygous neurons. (*M*) Quantification reveals a significant reduction of β-*actin* mRNA in distal dendrites of stau1^{tm1Apa} homozygous mice ($P < 0.001$). (*N*) Neurons were probed with oligo(dT) to detect polyadenylated mRNA and quantified as described. Significant reductions of mRNA particles in dendrites of neurons lacking Stau1 were detected both proximally (*, $P < 0.05$) and distally (**, $P < 0.01$). (Scale bars: 10 μm.)

dimerize (11). We therefore postulate that this dendritic localization of ΔStau1-EYFP in the WT background arises via a possible protein-protein interaction between WTStau1 and ΔStau1-EYFP. Since ΔStau1-EYFP no longer localizes in dendrites of neurons derived from ΔStau1 mice, this suggests that the dsRBDs might be, at least in part, involved in dimerization. We also noticed apparent differences in the intracellular localization of ΔStau1-EYFP in glia (Fig. S2*B*). In contrast to its typical ER association, ΔStau1-EYFP, although much less expressed in glia, shows a disrupted localization pattern.

We next investigated whether the formation and/or delivery of RNA-containing particles is impaired in neurons derived from stau1^{tm1Apa} homozygous mice. *In situ* hybridizations for β-*actin* mRNA show a small but significant reduction in the number of distal dendritic mRNA particles (Fig. 2 *K–M*): we found an average of 4.6 ± 0.8 β-*actin* mRNA particles per distal dendrite of WT neurons in contrast to 1.6 ± 0.5 ($P < 0.001$) in stau1^{tm1Apa} neurons. Similar observations were made using an oligo(dT) FISH probe to detect polyadenylated mRNA (Fig. 2*N*). Furthermore, employing real-time PCR, we found small but significant changes in the amount of β-*actin* mRNA compared to *GAPDH* mRNA in stau1^{tm1Apa}-derived neurons (0.71 fold change, $P < 0.01$). Taken together, our data suggest that Stau1 is involved in dendritic β-*actin* mRNP delivery. However, it is important to note that β-*actin* mRNA may not be specifically affected, since we observed changes in polyadenylated mRNA levels in dendrites of stau1^{tm1Apa} neurons by FISH as well as for α-*tubulin* mRNA by real-time PCR (data not shown). Further work is needed to investigate which other RNAs are specifically affected by loss of Stau1.

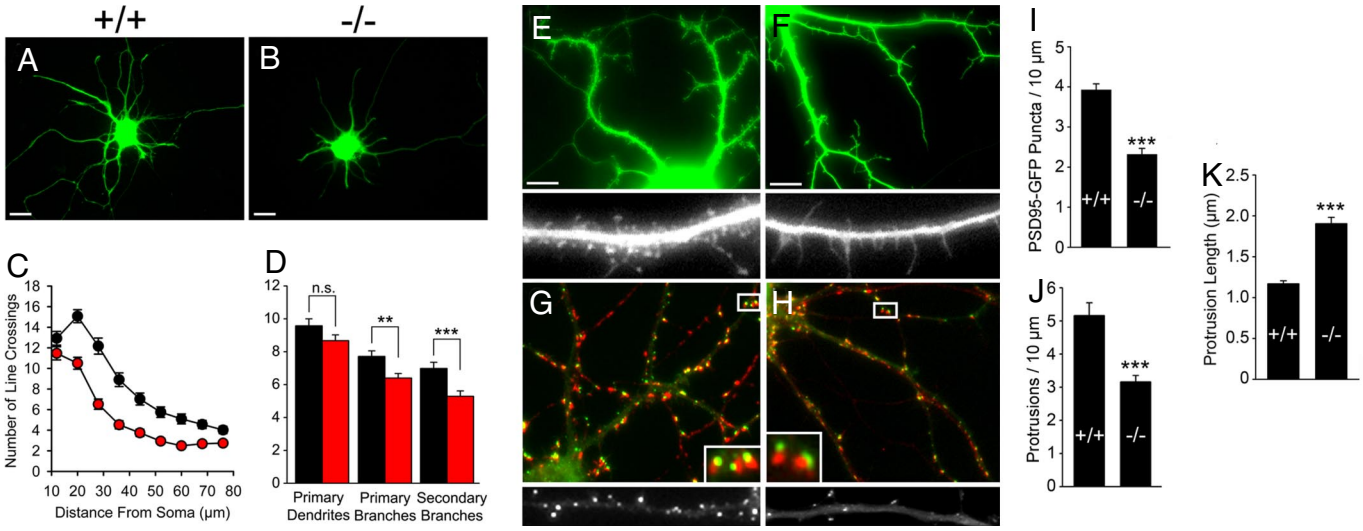

Fig. 3. Neurons lacking WTStau1 show impaired dendritic outgrowth and dendritic spine formation. WT mouse neurons are displayed on the left (*A, E,* and *G*) and those from stau1^{tm1Apa} homozygous mice are displayed on the right (*B, F,* and *H*). (*A, B, C,* and *D*) 7 DIV neurons derived from stau1^{tm1Apa} homozygous mice display impaired dendritic outgrowth and branching. (*C*) Sholl quantification of neurons lacking WTStau1 demonstrates significantly ($P < 0.001$) less complexity at distances greater than 21 μm from the center of the cell soma. 14 μm from the cell soma, no significant differences were detected. Quantification of primary dendritic outgrowth as well as primary and secondary branch points indicates primary dendrite number is unaffected. The stau1^{tm1Apa} homozygous mice demonstrate significantly fewer primary branch points ($P < 0.01$) and significantly fewer secondary branch points ($P < 0.001$) as compared to WT dendrites. (*E, F, J,* and *K*) 18 DIV mature neurons lacking Stau1 show alterations in dendritic spine morphology and density. Two representative neurons from WT (*E*) and stau1^{tm1Apa} homozygous mice (*F*) are shown with one overview (green) and one enlargement (gray scale) of a dendrite from another neuron. (*J* and *K*) Quantification reveals that mature neurons from stau1^{tm1Apa} homozygous mice form significantly fewer protrusions ($P < 0.001$, $\pm$ SE) than WT neurons (*J*) and that these protrusions are significantly longer in length as compared to WT protrusions (*K*; $P < 0.001$, $\pm$ SE). (*G, H,* and *I*) Neurons lacking WTStau1 have significantly fewer synapses ($P < 0.001$) and less presynaptic input. (*G* and H) Synapses were visualized via transfection with PSD95-GFP (green) followed by immunocytochemistry for the presynaptic protein synapsin (red). Enlarged insets show that these two markers are in close proximity indicating functional synapses. High magnifications below show dendrites from another neuron expressing PSD95-GFP. (*I*) Quantification of *F* and *G* reveals a significant reduction in synapse numbers ($P < 0.001$, $\pm$ SE). (Scale bars: 10 μm.)

Neurons Lacking WTStau1 Show Impaired Dendritic Outgrowth and Dendritic Spine Formation. Hippocampal neurons in culture develop in a stereotypical manner, both morphologically and temporally. During the initial culturing of neurons derived from both WT and stau1^{tm1Apa} homozygous mice, impairments in dendritic outgrowth were apparent. To visualize and quantify this phenotype, neurons were transfected with EGFP at 7 days *in vitro* (DIV) and fixed 18 h later. Sholl analysis was then performed on ≈60 neurons from 3 independent cultures. *Stau1*^{tm1Apa} homozygous neurons (Fig. 3*B* and red circles and boxes in Fig. 3 *C* and *D*) demonstrated significantly ($P < 0.001$) less dendritic complexity at distances greater than 21 μm from the center of the cell soma when compared to WT neurons (Fig. 3*A* and black circles and boxes in Fig. 3 *C* and *D*). Interestingly, primary dendrite number appears to be unaffected (9.6 $\pm$ 0.42 SE versus 8.7 $\pm$ 0.35 SE). However, neurons derived from stau1^{tm1Apa} homozygous mice displayed significantly fewer primary (7.7 $\pm$ 0.34 versus 6.4 $\pm$ 0.27, $P < 0.01$) and secondary (7.0 $\pm$ 0.38 versus 5.3 $\pm$ 0.32, $P < 0.001$) dendritic branch points as compared to WT neurons (Fig. 3*D*). This was the first experimental evidence that neurons lacking WTStau1 show deficits in dendritic length and branching during development.

It has recently been reported that downregulation of Stau1 via RNAi leads to changes in spine morphology in hippocampal slice cultures (15). Since the loss of Stau2 *in vitro* results in changes in dendritic spine morphology (9), we next assessed whether this impairment in dendritic targeting of the ΔStau1 protein leads to a similar phenotype in neurons derived from stau1^{tm1Apa} homozygous mice. Eighteen DIV, EGFP-transfected neurons were analyzed after 18 h for protrusion density and morphology (Fig. 3 *E* and *F*). Neurons derived from *stau1*^{tm1Apa} homozygous mice had a significantly lower ($P < 0.001$) protrusion density of 3.16 compared to 5.15 per 10 μm for WT mice (Fig. 3 *E, F, J*). Also, a change in morphology was observed. Although neurons lacking WTStau1 exhibited the stereotypical mushroom shaped dendritic spines (Fig. 3*E*), they had a higher ratio of long, thin filopodia-like structures (see also Fig. S4). Neurons derived from WT mice had protrusions of an average length of 1.17 μm, whereas neurons derived from *stau1*^{tm1Apa} homozygous mice had significantly longer protrusions (Fig. 3*K*, 1.90 μm, $P < 0.001$). This morphological phenotype is reminiscent of that found in neurons that have had Stau1 downregulated via RNAi (15) and of neurons lacking Stau2 (9). As stated, we observed a reduction in protrusion density in neurons lacking Stau1. This was not observed in Lebeau *et al.* (15). We can only postulate that this difference arises from the two experimental approaches used.

Next we determined whether neurons derived from stau1^{tm1Apa} homozygous mice were lacking presynaptic input. Both WT and stau1^{tm1Apa} homozygous-derived neurons were transfected with postsynaptic density protein-95 fused to GFP (PSD95-GFP) followed by immunostaining for the presynaptic protein synapsin 18 h later. Neurons lacking WTStau1 showed significantly less ($P < 0.001$) PSD95-GFP dendritic puncta compared to their WT counterparts (2.32 versus 3.92 per 10 μm of dendrite length) (Fig. 3*I*). However, all transfected PSD95-GFP puncta were still adjacent to presynaptic synapsin as observed in WT neurons (Fig. 3 *G* and *H Insets*). This indicates that although protrusion density is lower in neurons lacking WTStau1 and that their protrusion morphology is altered, they still retain the ability to form functional synapses as defined by both pre- and postsynaptic components found in close proximity. Further work will aim at identifying the electrophysiological properties of neurons derived from both genotypes.

Homozygous *stau1*^{tm1Apa} Mice Exhibit Intact Hippocampus-Dependent Learning but Decreased Locomotor Activity. To determine whether alterations in RNP localization, dendritic outgrowth and spine

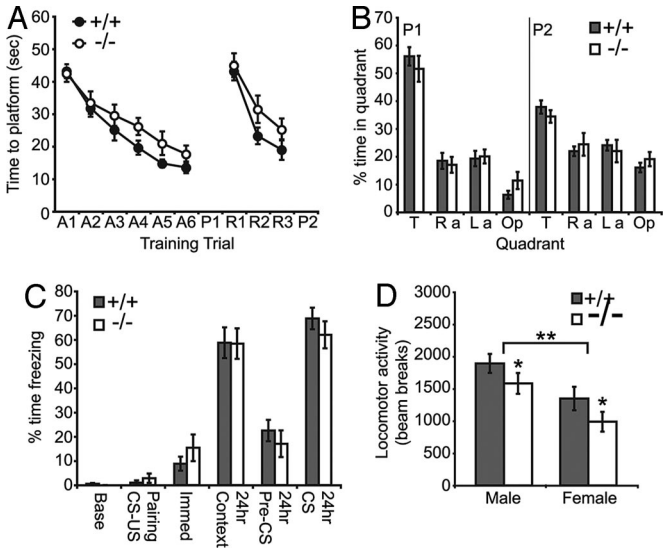

Fig. 4. Mice lacking WTStau1 exhibit intact hippocampus-dependent learning but decreased locomotor activity in the open field test. (*A*) In the Morris water maze, homozygous *stau1*^{tm1Apa} mice (n = 17) and WT littermates (n = 20) were trained over multiple days to find a hidden platform at an initial location (acquisition, A1–6) and at a new location on the opposite side of the pool (reversal, R1–3). Escape latency decreased across training trials and did not differ significantly between genotypes. (*B*) No significant difference between genotypes in preference for the quadrant of the water maze (Ra, right adjacent; La, Left adjacent; Op, opposite) that previously contained the hidden platform (T, target) during probe trials (P1–2). (*C*) No significant difference in freezing behavior between genotypes. In fear conditioning, homozygous *stau1*^{tm1Apa} (n = 13) mice and WT littermates (n = 17) learned to associate an unconditioned stimulus (US), a foot shock, with an auditory conditioned stimulus (CS) and the conditioning chamber itself (Context). (*D*) In the open field test, homozygous *stau1*^{tm1Apa} (n = 19, 9 males and 10 females) and WT littermates (n = 21, 12 males and 9 females) were placed in an automated open field apparatus for 30 min and activity was recorded. Female mice showed less activity overall and homozygous *stau1*^{tm1Apa} mice of both sexes exhibited significantly reduced activity than WT littermates. *, $P < 0.05$; **, $P < 0.01$.

formation in hippocampal neurons from homozygous *stau1*^{tm1Apa} mice translated to behavioral impairments, we tested these mice in two commonly used tests of hippocampus dependent learning and memory, the Morris water maze and contextual fear conditioning. In the water maze, both B6/stau1^{tm1Apa} homozygous mice (n = 17) and WT littermates (n = 20) demonstrated decreased escape latency over six training days (Fig. 4*A*, $F_{5,165}$ = 34.15, $P < 0.001$) and rapid acquisition of a new platform position during reversal learning ($F_{2,66}$ = 41.61, $P < 0.001$). There was no significant difference in escape latency between genotypes during learning trials or in preference for the quadrant of the pool that previously contained the platform when it was removed during probe trials (Fig. 4*B*). To increase sensitivity for learning deficits, we trained a separate cohort with two trials per day instead of four but again found no significant genotype difference (data not shown). In fear conditioning, mice learn to associate an aversive stimulus, a foot shock, with an auditory cue and a context, the conditioning chamber in which the shock occurred. Both B6/stau1^{tm1Apa} homozygous mice (n = 13) and WT littermates (n = 17) exhibited contextual and cued freezing (Fig. 4*C*, $F_{5,140}$ = 113.12, $P < 0.001$, posthoc $P < 0.001$ for context and cued), but there was no significant difference in the level of freezing between genotypes. The lack of a deficit in hippocampal function may reflect compensatory changes involving other proteins or genetic background effects. Notably, behavioral deficits in hippocampus dependent tasks have been subtle, absent, or inconsistent in mice lacking other components of neuronal RNPs such as FMRP (16, 17), BC1 (18), and translin (19), but changes in locomotor activity or anxiety-related behavior have been observed in all of these mouse models. To assess locomotor activity, we tested B6/stau1^{tm1Apa} homozygous mice (n = 19, 9 males and 10 females) and WT littermates (n = 21, 12 males and 9 females) in an automated open field activity chamber. Female mice exhibited significantly less activity overall (Fig. 4*D*; $F_{1,35}$ = 11.34, $P < 0.01$), and taking this difference into account, stau1^{tm1Apa} homozygous mice exhibited significantly less activity than WT littermates ($F_{1,35}$ = 4.37, $P < 0.05$). There was not a significant difference in anxiety-related behavior in the open field test or in another test of activity and anxiety, the elevated zero maze (data not shown).

In summary, we have generated a loss of function allele in murine *Stau1* using gene targeting to determine whether the lack of Stau1 affects neuronal granule assembly, synapse formation or learning and memory. Although no significant deficit in learning and memory could be observed, we did observe deficits in locomotor activity. There still remains the possibility of a subtle deficit in learning and memory yet to be detected. In culture, hippocampal neurons derived from *stau1*^{tm1Apa} homozygous mice display deficits in Stau1-containing RNP delivery to dendrites. Furthermore, these Stau1-deficient neurons have a significantly reduced dendritic tree and develop fewer synapses. Our data suggest that Stau1, as recently shown for Stau2, is crucial for synapse development *in vitro* but not critical for normal behavioral function.

Materials and Methods

Generation of stau1^{tm1Apa} Homozygous Mice. For all primer sequences used, see Table S1. To generate the targeting construct (Fig. 1*A*), a cassette containing IRESβgeo (20) was inserted into the BglII site of exon 5 in a subgenomic clone derived from a 129 BAC library (Genome Systems). Electroporation and neomycin selection was carried out in 129SvEv embryonic stem cells (CCB). Clones were screened for the presence of correct targeting by Southern blotting with a 5′ probe and 3′ PCR as shown in Fig. 1*B*. Two correctly targeted clones were identified and transmitted to the germline. Founder animals were initially backcrossed twice to 129SvEv WT mice before intercrossing for viability analysis. Mice used in the behavioral studies were the product of two backcross generations, two to 129 SvEv and subsequently two to C57Bl6/J WT mice. DNA extraction and Southern blot hybridization were performed as described (21). In brief, 10 μg of genomic DNA were digested with EcoRI (Fermentas). Genotyping of the mice was determined by using an [α-^{32}P]dCTP-radiolabeled Stau1 probe that has been generated with the Prime-It RmT random primer labeling kit (Stratagene) according to the manufacturer's protocol. This 5′ probe contains stau1 exons 1 and 2 located 5′ to the site of homologous recombination (nt 325–568, see Fig. 1*A*).

Cloning, RT-PCR, and Real-Time PCR. The cDNAs were amplified using the primers described in Table S1. To express EYFP-tagged Stau1, PCR products were cloned into the pEYFP-N1 expression vector (Clontech). To express untagged Stau1, the same vector without EYFP was used. All constructs were subsequently sequenced. An RT-PCR was performed on total RNA isolated from brain of WT, heterozygous, or mutant mice using the RNeasy Kit (Qiagen) according to the manufacturer's protocol. For real-time PCR, total RNA from 18 DIV WT and stau1^{tm1Ap} hippocampal neurons was isolated using TRIzol (Invitrogen) and cDNA was amplified using M-MLV reverse transcriptase (Promega) according to the manufacturer's instructions. GAPDH was used as control. Quantitative RT-PCR was performed using an iQ SYBR Green with MyiQ (both Bio-Rad). The reactions were performed in 25 μl final volume containing: iQ SYBR Green Supermix (Bio-Rad), 0.5 U TaqDNA Polymerase (Fermentas), forward and reverse primers (5 μM, Table S1). Changes in expression of *β-actin* RNA were related to the expression of *GAPDH* according to the $\Delta\Delta$Ct method. Experiments were repeated three times with RNA isolated from independent cultures. Data were tested for significance using a Student's t test and considered significant if $P < 0.05$.

FISH was essentially performed as previously described (22). Modifications are provided in the *SI Materials and Methods*. The following RNA probes were used: β-actin (NM_031144), nt 221–740 antisense and sense probes; histone H3.3 (X73683), antisense against full length.

Cell Cultures and Transient Transfections. Mouse hippocampal neurons were cultured and transiently transfected as described (23). HeLa cells were cultured in DMEM supplemented with 10% of FCS and were transfected using the Transfast Transfection Reagent (Promega) according to the manufacturer's instructions.

Western Blotting and Northwestern Assay. For Western blots, the following antibodies were used: immunopurified polyclonal rabbit anti-Stau1 and anti-Stau2 (both at 1:2,000) and monoclonal mouse anti-alpha tubulin (1: 5,000; Sigma). HeLa cells were transiently transfected with constructs expressing either WT or mutant untagged Stau1. After cell lysis, an RNA-binding assay was performed as described (14). After stripping, the membrane was then re-incubated with the immunopurified polyclonal Stau1 for Western blots analysis.

ACKNOWLEDGMENTS. We thank Barbara Grunewald, Sabine Thomas, and Martina Schwarz for excellent technical assistance. We are grateful to the following people for reagents and advice: Ulrich Eisel, Hans Lassmann, and D. St Johnston. This work was supported by the SFB446 (University of Tübingen, Germany), the Schram-Foundation, two HFSP networks, the Max-Planck-Society, an initial start-up grant from the MUW through Wolfgang Schütz (all to MAK) and by two grants from the Austrian Science Fund (FWF) to MAK and PM. SAJA was supported by a Wellcome Trust Career Development Fellowship. TA and JS were supported by the HFSP and the NIH.

1. Klann E, Dever TE (2004) Biochemical mechanisms for translational regulation in synaptic plasticity. *Nat Rev Neurosci* 5:931–942.
2. Sutton MA, Schuman EM (2006) Dendritic protein synthesis, synaptic plasticity, and memory. *Cell* 127:49–58.
3. Schüpbach T, Wieschaus E (1986) Germline autonomy of maternal-effect mutations altering the embryonic body pattern of Drosophila. *Dev Biol* 113:443–448.
4. St Johnston D, Beuchle D, Nüsslein-Volhard C (1991) Staufen, a gene required to localize maternal RNAs in the Drosophila egg. *Cell* 66:51–63.
5. Dubnau J, *et al.* (2003) The staufen/pumilio pathway is involved in Drosophila long-term memory. *Curr Biol* 13:286–296.
6. Kim YK, Furic L, Desgroseillers L, Maquat LE (2005) Mammalian Staufen1 Recruits Upf1 to Specific mRNA 3′UTRs so as to Elicit mRNA Decay. *Cell* 120:195–208.
7. Kim YK, *et al.* (2007) Staufen1 regulates diverse classes of mammalian transcripts. *EMBO J* 26:2670–2681.
8. Tang SJ, Meulemans D, Vazquez L, Colaco N, Schuman E (2001) A role for a rat homolog of staufen in the transport of RNA to neuronal dendrites. *Neuron* 32:463–475.
9. Goetze B, *et al.* (2006) The brain-specific double-stranded RNA-binding protein Staufen2 is required for dendritic spine morphogenesis. *J Cell Biol* 172:221–231.
10. Brizard F, Luo M, Desgroseillers L (2000) Genomic organization of the human and mouse stau genes. *DNA Cell Biol* 19:331–339.
11. Ramos A, *et al.* (2000) RNA recognition by a Staufen double-stranded RNA-binding domain. *EMBO J* 19:997–1009.
12. Maltais LJ, *et al.* (2002) Rules and guidelines for mouse gene, allele, and mutation nomenclature: A condensed version. *Genomics* 79:471–474.
13. Mallardo M, *et al.* (2003) Isolation and characterization of Staufen-containing ribonucleoprotein particles from rat brain. *Proc Natl Acad Sci USA* 100:2100–2105.
14. Wickham L, Duchaine T, Luo M, Nabi IR, DesGroseillers L (1999) Mammalian staufen is a double-stranded-RNA- and tubulin-binding protein which localizes to the rough endoplasmic reticulum. *Mol Cell Biol* 19:2220–2230.
15. Lebeau G, *et al.* (2008) Staufen1 regulation of protein synthesis-dependent long-term potentiation and synaptic function in hippocampal pyramidal cells. *Mol Cell Biol* 28:2896–2907.
16. Bakker CE, *et al.* (1994) Fmr1 knockout mice: a model to study fragile X mental retardation. The Dutch-Belgian Fragile X Consortium. *Cell* 78:23–33.
17. Peier AM, *et al.* (2000) (Over)correction of FMR1 deficiency with YAC transgenics: Behavioral and physical features. *Hum Mol Genet* 9:1145–1159.
18. Lewejohann L, *et al.* (2004) Role of a neuronal small non-messenger RNA: Behavioural alterations in BC1 RNA-deleted mice. *Behav Brain Res* 154:273–289.
19. Stein JM, *et al.* (2006) Behavioral and neurochemical alterations in mice lacking the RNA-binding protein translin. *J Neurosci* 26:2184–2196.
20. Bonaldo P, Chowdhury K, Stoykova A, Torres M, Gruss P (1998) Efficient gene trap screening for novel developmental genes using IRES beta geo vector and in vitro preselection. *Exp Cell Res* 244:125–136.
21. Southern E (2006) Southern blotting. *Nat Protoc* 1:518–525.
22. Wilkie GS, Davis I (1998) Visualizing mRNA by *in situ* hybridization using 'high resolution' and sensitive tyramide signal amplification. *Technical Tips Online* 3:94–97.
23. Goetze B, Grunewald B, Kiebler MA, Macchi P (2003) Coupling the iron-responsive element to GFP—An inducible system to study translation in a single living cell. *Sci STKE* 2003:PL12.